

INVESTIGATION OF A PHASE TRANSITION IN NICKEL WITH POLARIZED NEUTRONS

G. M. DRABKIN, E. I. ZABIDAROV, Ya. A. KASMAN, and A. I. OKOROKOV

A. F. Ioffe Physico-technical Institute, USSR Academy of Sciences

Submitted August 23, 1968

Zh. Eksp. Teor. Fiz. 56, 478-488 (February, 1969)

The region near the Curie temperature in nickel is investigated with the aid of polarized neutrons. The Curie point is determined with an accuracy of $\pm 1.3 \times 10^{-5}$ on the basis of neutron depolarization at $H = 0$. It is shown that measurement of the polarization of the transmitted beam is an effective means for investigating ferromagnets. A new method is proposed for measuring the induction in a sample with the aid of polarized neutrons. The temperature dependence of the magnetic susceptibility for $T > T_C$ is determined for $(T - T_C)/T_C$ lying between 5×10^{-5} and 4×10^{-3} . The scattering of neutrons with $\lambda \approx 5 \text{ \AA}$ by a nickel single crystal is measured for angles in the 6.8 to 67 minute range. It is shown that scattering near T_C can be divided into two types. One is scattering by long-range fluctuations existing at a temperature $|T - T_C| \sim 1^\circ\text{C}$, and the other is scattering observed at $-10 < T_C - T < +100^\circ\text{C}$. The first type of scattering is very sensitive to the magnetic field and disappears at angles $> 1^\circ$. The temperature position of the maximum of this scattering is constant at all angles and coincides with T_C with an accuracy of $\pm 0.1^\circ\text{C}$. The peak of the second type of scattering is at $T < T_C$ and shifts towards T_C with increasing scattering angle. The width of this scattering peak decreases on approaching T_C . A low-angle scattering peak is also observed at $T \sim 100^\circ\text{C}$.

1. INTRODUCTION

THIS work is a continuation of the study of the second-order phase transition in nickel by means of polarized neutron scattering. The first results were published in^[1] where it was shown that the scattering of neutrons in the direct vicinity of T_C is quasi-elastic. The purpose of this work is a further, more careful investigation of the small-angle critical neutron scattering by using the polarization effects of the scattering and by comparing the micro- and macroscopic characteristics of one and the same sample.

2. EXPERIMENTAL SETUP

The work was carried out on a VVR-M reactor on an installation described in^[2]. For this work the installation was partly modernized. The polarized neutron beam ($\lambda \sim 5 \text{ \AA}$, the polarization after reflection from the analyzer $P = P_p P_a = 70$ percent, and the cross section of the beam at the sample was 18×3 mm) was obtained by reflection from a magnetized iron mirror with a polarization $P_p \approx 84$ percent (1 on Fig. 1) and was analyzed by the same type of mirror 2 with $P_a \approx 84$ percent. The device 3 which made it possible to reverse the spin of the neutron with respect to the leading magnetic field nonadiabatically was constructed of two coils 60 mm in diameter. The distance between the coils was 400 mm. The coils were placed in a permalloy magnetic shield and produced opposing magnetic fields directed along the axis of the neutron beam. The efficiency of spin reversal by such a device $f \approx 100$ percent. The reversing devices were located before and after the sample. Since the directions of the magnetic fields in the polarizer, in the region of the sample, and in the analyzer were perpendicular to the direction of the incident beam, there were four regions in which the field direction changed. A test showed that the neutrons passed through these regions

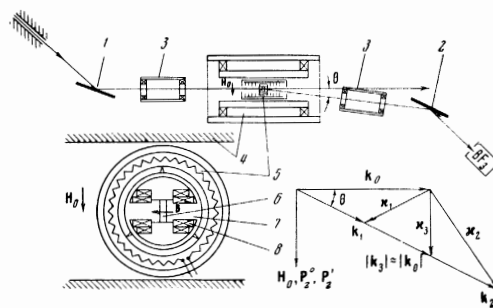


FIG. 1. Experimental installation and the kinematic diagram of the experiment. θ - scattering angle, k_0 and k_1, k_2, k_3 - wave vectors of the incident and scattered neutrons, H_0, P_z^0, P_z^1 - magnetic field vectors and the polarization of the incident and scattered neutrons.

adiabatically and with a depolarization less than 1 percent.

The leading field H_0 in the region of the sample was produced by the electromagnet 4 which was 800 mm long along the beam and between whose poles a non-magnetic furnace 5 with the sample 6 was located. The yoke of the magnet 4 (a cylinder 400 mm in diameter and 1000 mm long) served simultaneously as a magnetic shield against stray magnetic fields. The leading magnetic field H_0 was ~ 0.1 Oe. The magnet could be rotated about the beam axis setting the direction of the polarization vector $P_0 \parallel H_0$ of the incident neutrons (for convenience here and below we take P_0 to be the polarization measured in the absence of the sample, although the true $P_0 = P_p$).

The components of the vacuum furnace 5 were made of brass, copper, stainless steel and molybdenum. The insulation of the heat winding, the thermocouples, and of the platinum resistance thermometer was quartz. Three thermocouples were placed on the sample 6 (one gold-platinum and two copper-constantan ones) to regu-

late and measure the temperature, and two differential copper-constantan thermocouples to measure temperature gradients. An electromechanical stabilization system insured a temperature stability of $\Delta T = \pm 0.003^\circ$ during the entire time of measurement, and when required $\Delta T < 0.001^\circ$ for several hours.

The sample was placed between pole pieces closing the magnetic circuit of the ring electromagnet 7 made of Permendur. The diameter of the ring yoke was 40 mm and its width 20 mm. The total cross section of the magnetic circuit was 1 cm^2 . The pole pieces were prepared in accordance with the sample dimensions individually for each investigated sample. After completion the Permendur magnet was annealed in vacuum at $T = 800^\circ\text{C}$. In order to exclude any residual magnetization in polarization measurements of the transmitted beam in a field $H \sim 0$ and before each measurement of field-dependent effects, the magnet was demagnetized by alternating current which decreased smoothly to zero. The magnet produced a horizontal field perpendicular to the direction of the incident beam (Fig. 1). In measurements of the rotation of the polarization vector of the neutrons transmitted through the sample the leading field H_0 was vertical, i.e. perpendicular to the field in the sample.

The magnetic field H in the sample was not measured specially for each case but was estimated from the number of ampere-turns calibrated according to H for the case when the sample was taken out from the gap of the magnet. There is in fact no proportionality between H and the number of ampere-turns n_i , since the sample closed a magnetic circuit and the field H depended on the magnetic resistance of the sample. The correction can be estimated from the magnetic circuit equation

$$0.4\pi n_i = H\Delta l_1 + H_2\Delta l_2 = \frac{\Phi\Delta l_1}{(1 + 4\pi\chi)S_1} + \frac{\Phi\Delta l_2}{\mu_2 S_2}. \quad (1)$$

Here Φ is the magnetic flux, Δl_1 and Δl_2 are the dimensions of the sample and magnetic circuit along the magnetic lines of force, S_1 and S_2 are the cross sectional areas of the sample and of the magnetic circuit, χ is the susceptibility of the sample, and μ_2 is the permeability of the magnetic circuit. In our conditions the discrepancy between the field and the number of ampere-turns did not exceed 3 percent for the temperature region $|T - T_c| \sim 5^\circ$.

3. DETERMINATION OF T_c

The polarization P of the neutron beam which has passed through the crystal contains information about the fluctuations of the magnetic field along the neutron path in the sample. The domains in the ferromagnetic region ($T < T_c$) and the fluctuations of the magnetic density for $T > T_c$ in the vicinity of T_c give rise to random rotations of the neutron spin and depolarize the initially polarized neutron beam. For $H = 0$ the experimental $P(T)$ dependence falls steeply in the region of T_c (Figs. 2 and 3), the maximum slope coinciding with the critical scattering peak and with the susceptibility maximum. One can cite qualitative arguments pointing towards the fact that T_c coincides with the maximum of dP/dT .

Halpern and Holstein^[3] considered the depolariza-

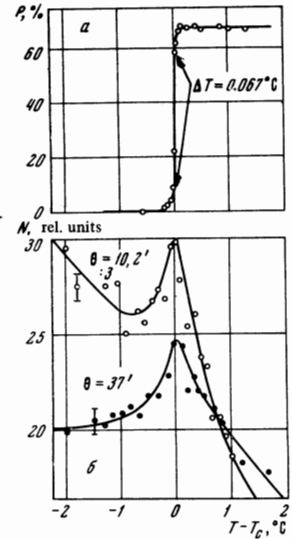


FIG. 2. Temperature dependence a— of the polarization of the transmitted beam for $H = 0-0.1 \text{ Oe}$ for a section of the nickel crystal, and b— for the intensity of the critical scattering at angles $\theta = 10.2'$ and $\theta = 37'$ (for $\theta = 10.2'$ the scale is decreased by a factor of three).

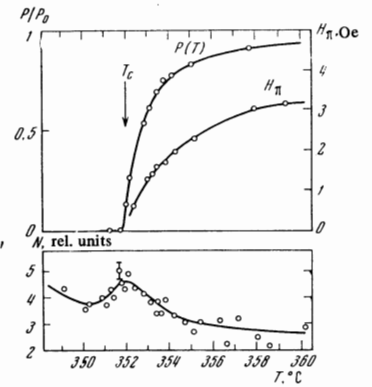


FIG. 3. The polarization of the transmitted beam P , the intensity of the magnetic field $H_\pi = 1/(1 + 4\pi\chi)$, and the critical scattering at an angle $\theta = 10.2'$ for polycrystalline nickel 20 mm thick.

tion of neutrons by domains. They derived for the depolarizing factor the relation:

$$\frac{P}{P_0} = \exp \left\{ \frac{1}{3v^2} g^2 \sum_i B_i^2 \delta_i^2 \right\}, \quad (2)$$

where g is the gyromagnetic ratio, v is the neutron velocity, P_0 and P is the polarization of the incident and transmitted beam, B_i is the magnetic field within the domain, and δ_i is the domain dimension. The sum is taken over all domains along the neutron path. This formula is correct for $gB_i\delta_i/2v \ll 1$. Near the Curie point for $T > T_c$ where the spontaneous magnetization is small this condition is obviously fulfilled. The general applicability of (2) for the region $T > T_c$ raises some objection, because the dimensions of the fluctuations and the magnetic fields in them change with time. One can, however, assume qualitatively that (2) is fulfilled for $T > T_c$. In this case B and δ refer to the average magnetic field and the average effective dimension of the fluctuations. Omitting the summation over i , it then follows from (2) that

$$\frac{dP}{dT} \sim P_0(-2c)B^2\delta^2 \left[\frac{dB}{dT} \frac{1}{B} + \frac{d\delta}{dT} \frac{1}{\delta} \right] \exp\{-cB^2\delta^2\}.$$

Assuming that in this formula, for instance in accord with the work of Kadanoff et al.,^[4]

$$\delta \sim \left| \frac{T - T_c}{T_c} \right|^{-\nu} \equiv \tau^{-\nu}, \quad \chi \sim \left| \frac{T - T_c}{T_c} \right|^{-\gamma} \equiv \tau^{-\gamma},$$

we obtain for the expression in brackets $-(\gamma + \nu)/\tau$. Then

$$\frac{dP}{dT} \sim P \frac{1}{\tau^{2\nu/(2\nu+1)}} \quad (3)$$

Thus, on approaching T_C the value of dP/dT tends to a maximum. A rigorous mathematical calculation of the polarization of the transmitted beam for $T \approx T_C$ would be of undoubted interest.

In all cases observed by us (Figs. 2–4) the section of the steep fall of the $P(T)$ curve coincides with the maxima of the critical scattering and susceptibility which correspond to T_C .^[5,6] The polarization curve thus localizes the region of determination of T_C with an accuracy up to hundredth parts of a degree (Fig. 2). By stipulating the choice of T_C from the maximum of dP/dT , one can obtain a considerable reproducibility of the Curie point.

We obtained the largest slope $dP/dT = 13 \text{ deg}^{-1}$ for a single crystal of nickel with a purity of $R(300^\circ\text{K})/R(4.2^\circ\text{K}) \approx 40$. This corresponds to a $\pm 0.008^\circ$ accuracy in the determination of T_C . The absolute value of $T_C \approx 622.3^\circ\text{K}$ was determined from a standard calibration of gold-platinum and copper-constantan thermocouples.

With increasing thickness of the sample and possibly increasing impurity the $P(T)$ curve spreads in the direction of higher temperatures (Fig. 3 for polycrystalline nickel 20 mm thick). However, in this case too the maximum of dP/dT coincides with the susceptibility maximum and with the maximum in the critical scattering of neutrons. It can be assumed that for samples of higher purity dP/dT would increase appreciably and the accuracy in the determination of T_C would increase. For comparison we note that the accuracy in the determination of T_C from an extrapolation to T_C from the region of large $|T - T_C|$, as well as from the maxima of the critical scattering and of the susceptibility is of the order of 10^{-4} . In our instance the uncertainty of T_C amounts to 1.3×10^{-5} .

4. THE EFFECT OF A MAGNETIC FIELD ON $P(T)$

Figure 5 shows the shift and change in the form of the polarization curve $P(T)$ on the external magnetic field H applied to the sample. The course of the $P(T)$ curve on the section a-b of curve 3 for a constant $H = 16 \text{ Oe}$ is most probably connected with processes of alignment of the moments of the domains with the field. The section b-c is similar to the corresponding section of the $P(T)$ curve for $H = 0$. Although the $P(T, H)$ curves have a smaller slope than $P(T, 0)$, they clearly exhibit a sharp drop analogous to that of the $P(T, 0)$ curve from which T_C was determined.

Let us introduce a temperature $T_1(H)$ for which $\partial P(T, H)/\partial T$ has a maximum, and let us plot its dependence on H (curve 4 in Fig. 5). The experimental points fit well the curve corresponding to the quadratic dependence:

$$T_1(H) = T_c - aH^2, \quad a = (2,3 \pm 0,3) \cdot 10^{-3} \text{ deg/Oe}^2. \quad (4)$$

The maximum observed shift of the polarization curve $\Delta T = T_C - T_1$ under the action of a field $H = 16 \text{ Oe}$ is 0.57°C . The nature of such a behavior of $P(T)$ is not clear. A check of the possible connection of the $P(T, H)$ shift with the shift of the peak of the critical

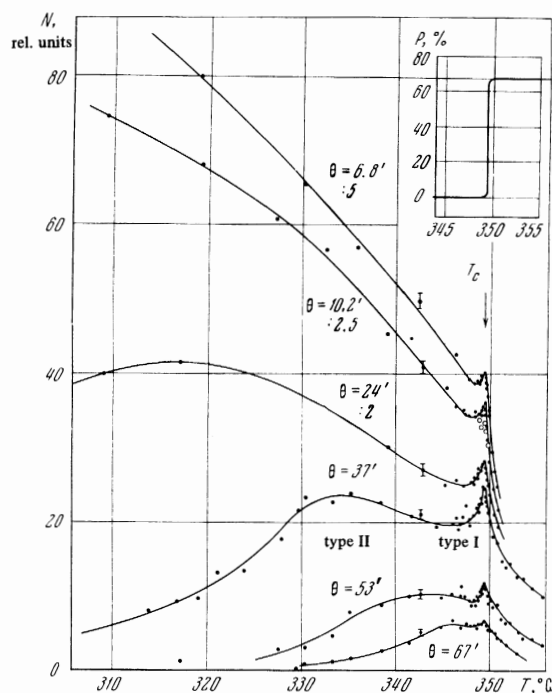


FIG. 4. Temperature dependence of the neutron scattering in nickel at the angles θ for $H \sim 0$. The open circles denote scattering with $H = 10 \text{ Oe}$ ($\theta = 10.2'$).

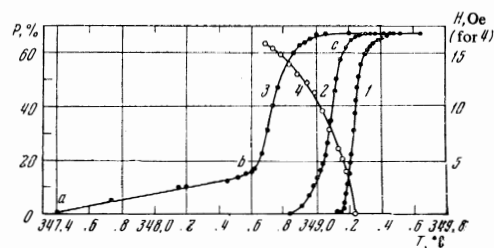


FIG. 5. The shift of the polarization curve $P(T)$ under the action of a magnetic field: 1 – $H = 0$, 2 – $H = 8 \text{ Oe}$, 3 – $H = 16 \text{ Oe}$; curve 4 – position of the maximum of the derivative $\partial P(T, H)/\partial T$ on the “field temperature” plane.

scattering of neutrons is difficult, since for small fields the shift is much smaller than the width of the peak and for large fields the peak of the critical scattering of the first kind (see Sec. 7) practically disappears.

A careful measurement of the $P(T, H)$ curves in the region of T_C and their comparison with other characteristics of the phase transition appears to us to be useful.

5. THE MAGNETIC INHOMOGENEITY OF THE FERROMAGNETIC SAMPLES

Probing the single-crystal sample of nickel with a fine beam of polarized neutrons (with a $1 \times 1 \text{ mm}$ cross section), we observed that the polarization curves $P(T)$ for various parts of the sample are appreciably shifted in temperature. This means that the value of T_C is not the same for different parts of the sample.

The experiment was carried out as follows. The sample with a cross section of 20×6 mm was covered with a shielding diaphragm made of a titanium-gadolinium alloy with a 18×4 mm opening. The temperature at which the polarization was $P_{\max}/2$ was established. The magnet and the sample were demagnetized by a decreasing alternating field for $T > T_c$ for nickel, and during the entire measurement $H \sim 0.1$ Oe. Furthermore the beam was covered by another shielding diaphragm with a 1×1 mm opening. A coordinate mechanism translated the diaphragm and made it possible to investigate the entire cross section of the uncovered part of the sample (18×4 mm) in 1-mm steps. The polarization of the transmitted beam was measured at each coordinate point. The results are presented in Fig. 6b.

For those regions in which the polarization had a maximum or vanished, the measurements were repeated at other temperatures for which the polarization in these regions corresponded to the steep section of the $P(T)$ curve. The results show that T_c determined from the largest slope of $P(T)$ differs by $\sim 0.5^\circ$ on various sections. The maximum possible temperature gradient over the sample is much smaller and is in addition of different sign. It is seen from the geometry of the device and the position of the heating elements (8, Fig. 1) that the temperature of the center of the sample cannot be lower than that at its edges. Additional thermal screening of the sample and a redistribution of the regulating heating elements did not change the pattern of the polarization inhomogeneity. The change of the form of the $P(T)$ dependence of the entire sample (curve 1 in Fig. 5) compared with the $P(T)$ of an individual section (Fig. 2a) is qualitatively similar to the change of the form of $P(T)$ under the action of a magnetic field (curves 2 and 3 of Fig. 5), which leads one to think of a magnetic nature of the sample inhomogeneity.

We note that the dependence of $P(T)$ on the coordinates of the sample reproduces approximately the contours of the grown single-crystal block from which the sample was cut (Fig. 6a). This inhomogeneity is possibly connected with technological features of the crystal growth. One can also assume that the scatter in T_c over the cross section of the sample (Fig. 6b) and the dependence of T_1 on the field H [Eq. (4)] are connected with the magnetization modes discussed in the work of Arrot.^[7] In this case T_1 takes on the meaning of $T_c(H)$. Such an inhomogeneity cannot be observed by other methods based on the investigation of various properties of ferromagnetic substances (magnetic and calorimetric properties, and the scattering of unpolarized neutrons). In connection with the inhomogeneity of our sample all the results presented in this article, with the exception of Figs. 3, 5, and 6, were obtained for the section of the sample with the coordinates $h = 11-16$ and $b = 0-2$ (Fig. 6b).

6. MEASUREMENT OF THE SUSCEPTIBILITY IN THE VICINITY OF T_c

In order to determine the magnetic susceptibility, we made use of the precession of the neutron spins

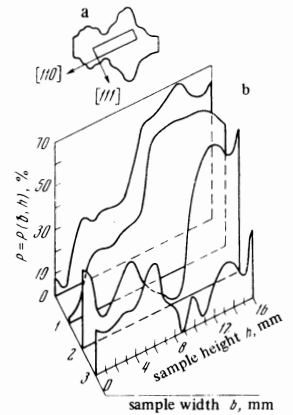


FIG. 6. The shape of the unprocessed single-crystal block of nickel (a) and the dependence of the polarization (b) of the transmitted beam on the coordinates of the sample (the mean polarization of the sample is 30 percent).

about the internal field of the sample B . Considering the classical equation of motion of the neutron spin^{[3]*}

$$\frac{ds}{dt} = [\mu B(r)] \frac{1}{\hbar} = g[sB(r)],$$

where s is the neutron spin in units of \hbar , μ is the magnetic moment of the neutron, B is the magnetic field in the sample, $g = 2\mu/\hbar$ is the gyromagnetic ratio of the neutron, it is seen that when the neutron passes through a region of magnetic field B the spin component s_{\parallel} parallel to B does not change, whereas the perpendicular component s_{\perp} precesses about B with an angular velocity $\omega = gB$. If a neutron with a velocity v is made to pass through a sample of dimension d in which a constant magnetic field $B \perp s_{\perp}$ is present, one can draw conclusions about the value of $B = v\varphi/gd$ from the angle φ through which the spin has been turned.

Let us introduce a polarized neutron beam with a polarization $P = P_z^0$ (the z axis is directed along the leading field H_0) nonadiabatically into the perpendicular magnetic field of the sample (Fig. 1). The P_z^0 component of the polarization will then become P_z^1 with respect to the field B . During the time of flight of the neutron through the sample the polarization vector will turn. If the neutrons are now nonadiabatically brought out into the previous leading magnetic field H_0 and if the z component of the polarization is measured, then

$$P_z^1 = P_z^0 \cos \varphi = P_z^0 \cos \left(g \frac{Bd}{v} \right). \quad (5)$$

If the internal field of the sample B is set by the external field H , then by measuring P_z^1 as a function of H , one can determine $B = H(1 + 4\pi\chi)$. The period of rotation of the polarization vector is then

$$H_{2\pi} = 2\pi vH / gB(H)d,$$

where $H_{2\pi}$ is the value of the external field for which the polarization vector rotates by an angle of 2π . This method has a reasonable sensitivity for $\chi \gtrsim 10^{-3}$, but its main advantage lies in the fact that it allows one to measure χ in small fields ($H \sim 0.5$ Oe for $\lambda_n \sim 10 \text{ \AA}$, $d \sim 1$ cm and for $\chi \sim 1$). This method is particularly convenient for measuring χ in the immediate vicinity of T_c , since $H_{2\pi} \sim 1/B$.

* $[\mu B(r)] \equiv \mu \times B(r)$.

In our experiments we fixed a given magnetic flux Φ_n which rotated the polarization vector by an angle of 180° , and noted the required number of ampere-turns $(ni)_\pi \approx H_\pi/0.4\pi$. Under these conditions Eq. (1) becomes

$$0.4\pi(ni)_\pi = \frac{c_1}{1 + 4\pi\chi} + c_2, \quad (6)$$

where c_1 and c_2 are constant coefficients:

$$c_1 = \frac{\Phi_\pi \Delta l_1}{S_1} = \frac{\pi v \Delta l_1}{g l}, \quad c_2 = \frac{\Phi_\pi \Delta l_2}{\mu_2 S_2}.$$

In Fig. 7 we present the susceptibility as a function of temperature calculated in accordance with Eq. 6. The magnetic field H applied to the sample was varied within the limits from zero to several oersted near T_C and from 0 to 10 Oe for $T - T_C \sim 3^\circ$. For these values of the field H we did not observe a dependence of χ on H , i.e. the first three or four periods of rotation of the polarization vector were equal (Fig. 8). We tried to represent the temperature variation of the susceptibility in the form $\chi = \tau^{-\gamma}$, and found that the experimental points follow a power dependence in the range of temperatures τ from 5×10^{-5} to 4×10^{-3} (Fig. 9). We refrain from an interpretation of this result, because in this temperature region the purity of the investigated material plays a decisive role and our sample is insufficiently pure.

The experimentally obtained dependence (5) is a damped cosine curve with a positive constant component (Fig. 8). The damping is due to the insufficient monochromaticity of the neutron beam. The angle of rotation of the spin depends on the neutron velocity and for a nonmonochromatic beam there is a phase difference $d\varphi = gB(H)v^{-2}dv$ which increases with increasing $B(H)$ and leads to a depolarization of the neutron beam. The constant component is apparently connected with the incomplete nonadiabaticity with which the neutrons cross the boundary of the crossed fields in the region of the sample and with the appearance in the polarization of a component parallel to the field B within the sample. A depolarization of the neutron

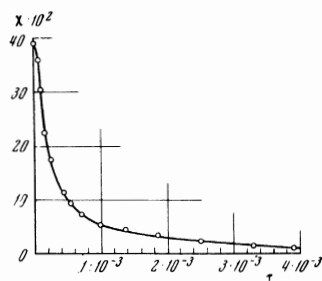


FIG. 7. The temperature dependence of the susceptibility for a single crystal of nickel [$\tau = (T - T_C)/T_C$].

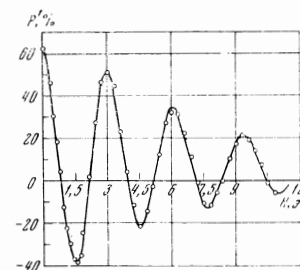


FIG. 8. Rotation of the polarization vector in the sample with the field H perpendicular to P_0 .

beam occurs on approaching T_C (Fig. 2a). This makes it impossible to measure the susceptibility for $T < T_C$. This difficulty can be avoided by passing the neutron beam not through the sample but through such a narrow gap in the sample that within it $H = B$. We hope that an improvement of the experimental conditions will allow us to follow the dependence of the magnetic susceptibility on the applied magnetic field H and to include the region $T < T_C$.

7. ANALYSIS OF THE DATA ON THE SCATTERING OF NEUTRONS AT VARIOUS ANGLES

In Fig. 4 we present the results of measurement of the scattering of polarized neutrons with $\lambda \approx 5 \text{ \AA}$ by a single crystal of nickel near the Curie point. On the scattering intensity-temperature curve one can distinguish two types of scattering.

The first type of scattering is connected with the scattering of neutrons in the immediate vicinity of T_C . The scattering maximum is at T_C and its position does not depend on the scattering angle. The distance decreases with increasing angle and is very sensitive to the magnetic field in which the sample is placed. It is sufficient to apply a field of 10 Oe for the scattering to disappear practically at angles $10.2' - 17'$ (Fig. 3, $\theta = 10.2'$).

The second type of scattering near T_C is represented by a considerably broader maximum. This scattering is less sensitive to the magnetic field and its peak is clearly manifested at considerably larger angles. The position of the maximum in this region of angles and temperatures depends on the scattering angle θ and with increasing θ approaches T_C .

The first type of scattering is apparently due to long-range order fluctuations in the transition of the sample from the paramagnetic to the ferromagnetic state. As has been shown in our preceding work^[1] this scattering is of a quasi-elastic nature¹⁾. The considerable inelasticity noted by the authors of^[10,11] apparently attests to the fact that they were measuring the

¹⁾ In this connection it must be noted that the statement by Riste et al. [8] to the effect that in small-angle scattering a change in the sign of the polarization of the neutrons does not indicate a quasi-elastic nature of the scattering but occurs whenever the polarization vector P_0 is parallel to the scattering vector κ , is apparently based on a misunderstanding. Obviously the authors have in mind the small-angle scattering near a reciprocal lattice vector $\kappa_0 \neq 0$. In this case the scattering vector $\kappa = k - k_0$ is fixed in the direction κ_0 . In our case $\kappa_0 = 0$ (Fig. 1) and in inelastic scattering (k_1 and k_2 , Fig. 1) the direction of the scattering vector κ (κ_1 and κ_2 in Fig. 1) is altogether not fixed relative to the polarization vector P_0 . Since P_0 is perpendicular to k_0 and lies in the same plane as κ , the scattering vector will turn out to be parallel to the polarization vector P_0 only in elastic small-angle scattering ($\kappa \equiv \kappa_3$, Fig. 1). It was this type of scattering which we observed near T_C of nickel for $T > T_C$ (paramagnetic phase) and from the change of sign of the polarization with its magnitude constant we drew the conclusion regarding the quasi-elasticity of the critical scattering in the immediate vicinity of T_C . A decrease of the absolute magnitude of the polarization with increasing temperature indicates an increase of the transferred momentum. Thus for $T - T_C > 1 - 2^\circ$ there appears in the critical neutron scattering a considerable elasticity (for details about this see the paper of Maleev [9]).

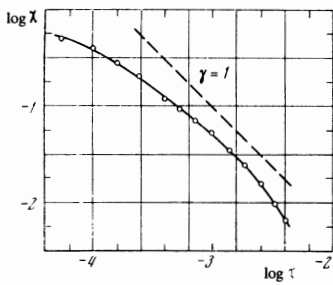


FIG. 9. Temperature dependence of the susceptibility for a single crystal of nickel ($\gamma = \log \chi / \log \tau$).

second type of scattering. From the scattering pattern of iron^[12] at angles of $0.92\text{--}3.02^\circ$ ($\lambda = 4.75 \text{ \AA}$) it is seen that here too there is a narrow peak which disappears in a magnetic field of 300 Oe (first type). The broad skirts of this peak (second type) have a maximum for $T < T_C$. On increasing the scattering angle this maximum approaches T_C . The shift of this maximum has apparently also been observed by Stump and Maier.^[13]

We have also observed the scattering by nickel in the $20\text{--}350^\circ\text{C}$ temperature range (Fig. 10). Here we have a broad scattering peak with a maximum in the region of 100°C which decreases with increasing scattering angle. This scattering is possibly connected with the nature of the domain walls, since the maximum corresponds to the temperature at which the anisotropy constant K_1 approaches zero. A magnetic field

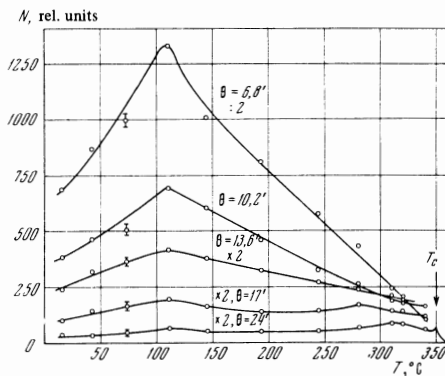


FIG. 10. Temperature dependence of the neutron scattering at the angles θ ($\times 2$, $\times 2$ — changes of scale).

of about 150 Oe decreases this scattering by a factor of four. This is accompanied by a decrease of the peak width and the maximum remains in the region of 100°C . The scattering observed by us should be the subject of a more careful additional investigation.

In conclusion the authors thank K. G. Voinova, V. I. Volkov, G. P. Didenko, V. N. Sumarokov, and A. F. Shchebetov for assistance in carrying out the measurements and in the construction of the apparatus. We note with pleasure the fruitful discussion of the results with S. V. Maleev and I. Ya. Korenblit and thank them for valuable advice and remarks. We are grateful to D. M. Kaminker for his continuous interest and assistance with the work.

¹G. M. Drabkin, E. I. Zabidarov, Ya. A. Kasman, and A. I. Okorokov, *ZhETF Pis. Red.* **2**, 541 (1965) [*JETP Lett.* **2**, 336 (1965)].

²G. M. Drabkin, E. I. Zabidarov, Ya. A. Kasman, A. I. Okorokov, and V. A. Trunov, *Zh. Eksp. Teor. Fiz.* **47**, 2316 (1964) [*Sov. Phys.-JETP* **20**, 1548 (1965)].

³O. Halpern and T. Holstein, *Phys. Rev.* **59**, 960 (1941).

⁴L. Kadanoff, W. Gotze, D. Hamblen, R. Hecht, E. A. S. Lewis, V. V. Palciauskas, M. Payl, and J. Swift, *Rev. Modern Phys.* **39**, 395 (1967).

⁵L. Van Hove, *Phys. Rev.* **95**, 249 (1954).

⁶K. P. Belov, *Magnitnye prevrashcheniya (Magnetic Transitions)*, Fizmatgiz, 1959.

⁷A. Arrot, *Phys. Rev. Letters* **20**, 1029 (1968).

⁸T. Riste, R. M. Moon, and W. C. Koehler, *Phys. Rev. Letters* **20**, 997 (1968).

⁹S. V. Maleev, *ZhETF Pis. Red.* **2**, 545 (1965) [*JETP Lett.* **2**, 338 (1965)].

¹⁰L. Passell, K. Blinowski, T. Brun, and P. Nilsen, *J. Appl. Phys.* **35**, 933 (1964).

¹¹J. Als-Nielsen, O. W. Dietrich, W. Marshall, and P. Lingörd, *Solid State Comm.* **5**, 607 (1967).

¹²B. Jacrot, J. Konstantinovic, G. Parette, and D. Cribier, *Inelastic Scattering of Neutrons in Solids and Liquids*, vol. **2**, IAEA, Vienna, 1963, p. 317.

¹³N. Stump and G. Maier, *Phys. Letters* **24A**, 625 (1967).

Translated by Z. Barnea